Iranian Journal of Analytical Chemistry
Volume 8, Issue 2, September 2021 (50-58) Origonal Research Article

مجله ایرانی شیمی تجزیه
دوره۸، شماره ۲، مهرماه ۱۴۰۰ (۵۸-۵۰)

Quantification of Hydrogen Peroxide in Milk Samples Based on Glassy Carbon Electrode Modified with Fe/Cu Layered Double Hydroxide and Fe_3O_4 Nanoparticles

Arefeh Gorgij[1], Hamid Ahmar[1,*], Laleh Adlnasab[2]
1. Department of Chemistry, Faculty of Science, University of Zabol, P. O. Box 98615-538, Zabol, I.R. Iran
2. Chemistry Research Group, Chemistry and Petrochemistry Research Center, Standard Research Institute, P.O. Box: 31745-139, Karaj, Iran
Received: 2 August 2021 **Accepted:** 16 September 2021
DOI: 10.30473/ijac.2022.62519.1217

Abstract
This research aimed to develop a novel sensing platform for hydrogen peroxide (H_2O_2) quantification in the milk samples. The proposed sensor was fabricated using a glassy carbon electrode modified with Fe-Cu layered double hydroxide (LDH)/magnetic Fe_3O_4 nanoparticles (FeCu-LDH@Fe_3O_4/GCE). The resulting sensor was characterized using field emission scanning, electron microscopy, x-ray diffraction, and infrared spectroscopy, with the addition of the electrochemical methods. After optimization of affecting parameters, the FeCu-LDH@Fe_3O_4/GCE exhibited a high electrocatalytic activity for H_2O_2 electroreduction; and high cathodic peak currents were obtained. The proposed electrode also illustrated a wide linear dynamic domain in the range of 2 to 400 µM; and low limit of detection was calculated to be 0.6 µM.

Keywords
Nanoparticles; Hydrogen Peroxide; Layered Double Hydroxides; Electrochemical Sensor; Milk Samples.

1. INTRODUCTION

Hydrogen peroxide (H_2O_2) has various applications in different areas of science such as environmental, pharmaceutical, clinical, and industrial research and has high antibacterial, and oxidizing characteristics [1-3]. However, H_2O_2 could simply move and be accumulated in the environment, especially in atmosphere, and in water supplies [4]. This can give rise to the formation of hazardous and dangerous H_2SO_4 and HNO_3, and excessive presence of these acids could lead to enhancement of rain acidity level; consequently, it can result in reduction of pH of water resources. H_2O_2 is also a well-known by-product of oxidases biochemical reactions which is regarded as a marker for oxidative stress, and acts as a signaling molecule and defense agent as well [2-4]. Also, according to recent research, H_2O_2 can lead to a diverse range of diseases such as Alzheimer's, Cancer, and Diabetes. In addition, drinking water, which contains the H_2O_2, can affect human health and result in vomiting, dizziness, and nausea [3, 4]. As a result, development of a sensitive analytical method is important to quantify the H_2O_2 concentration in different real environments.

Several reports have been published for determination of H_2O_2 such as chemiluminescence [5, 6], colorimetric [7], chromatography, optical spectroscopy [8], and other methods on the basis of electrochemistry [9-12]. In the last few decades, electrochemical approaches have been considered the strategies of choice due to their simplicity, sensitivity and low costs [13]. Regarding the previously reported methods, electrochemical sensors for determination of H_2O_2 are mainly on the basis of biomaterials such as Hemoglobin, Horseradish Peroxidase, and Myoglobin as biorecognition elements. These biosensors have been widely used for selective and sensitive quantification of H_2O_2 [1, 11, 14, 15]. However, although these sensors provide good sensitivity and selectivity, some characteristics such as lack of thermal and chemical stability and low reproducibility of these electrodes due to complex immobilization steps have attracted great attention for determination of H_2O_2 on enzyme-free sensors [15]. As a result, a range of modified electrodes based on nanocomposites, containing metal nanoparticles and new inorganic structures, have been developed for H_2O_2 sensing [16].

Development of modified electrodes has gained great attention in the field of electrochemical sensors. The main goal of electrode modification is to catalyze and facilitate electron transfer process [16]. Due to unique properties of nanoparticles and

*Corresponding Author: h.ahmar@yahoo.com, h.ahmar@uoz.ac.ir

synthetic inorganic materials, which include low overpotentials and high electron transfer kinetics on the electrode surfaces, high specific surface area and high stability, they have been widely used for preparation of modified electrodes [12].

Layered double hydroxides (LDHs), widely recognized as hydrotalcite-like materials and/or anionic clays, account for a large number of interlayer charge balancing anions, positively charged hydroxide layers, and water molecules [17, 18]. LDHs have a large number of unique characteristics such as encapsulation ability, high catalytic activity, and ion exchange properties with selective shape [18]. LDHs has received great attention in recent years as promising materials due to their wide range of applications such as catalysts, ion exchanger materials, adsorbents, and electrode modifiers [19]. To explain how these materials can be used in trace level analysis, it should be considered that these materials help desired analytes be confined into an interlayer and small volume on the electrode surface during the analytical measurements [20, 21]. This can improve the results of analytical methods, especially detection limits (LODs). It is also of great importance that these materials can provide high surface area for immobilization of other electrocatalytic reagents to improve sensitivity and selectivity of the electrodes [20, 21]. Several reports have been published in the area of electrochemical sensors, based on LDHs in different biological and environmental applications [22, 23]. Magnetic nanoparticles (MNPs) have been used in different areas of analytical and biomedical applications. Examples of these studies include application of these active interfaces to fix biorecognition elements for labeling and detecting lignocellulose activity and gene expression [24, 25]. Iron oxide (Fe_3O_4) is particularly popular due to its conductivity, large specific surface area, facile synthesis, and its easy separation from solutions using a magnet [24, 25]. Incorporation of LDHs with Fe_3O_4 nanoparticles could improve surface area and conductivity of the modified electrodes, resulting in improvement of the electrochemical responses.

In this research, a nanocomposite synthesized from FeCu-LDH and Fe_3O_4 nanoparticles was used as electrode modifier for development of electrochemical H_2O_2 sensor. Finally, electrochemical behavior of FeCu-LDH@Fe_3O_4 modified electrode was studied for the electroreduction of H_2O_2 in real milk samples.

2. EXPERIMENTAL

2.1. Reagents

H_2O_2, HCl, NaOH, potassium hydrogen phosphate (K_2HPO_4), potassium dihydrogen phosphate (KH_2PO_4), Na_2CO_3, $CuCl_2.2H_2O$, $FeCl_3.6H_2O$ and $FeCl_2.4H_2O$ were purchased from Merck Company (Darmstadt, Germany) and used as received without any further purification. Also, tetraethyl orthosilicate (TEOS, 98% purity) was obtained from Sigma-Aldrich Company.

To preparation of phosphate buffer solution having pH of 7 and 0.1 M concentration, 15.487 g of $Na_2HPO_4.7H_2O$ and 5.827 g of $NaH_2PO_4.H_2O$ were dissolved in 800 mL of distilled water in a suitable container. Desired pH was adjusted with HCl or NaOH and then diluted with distilled water to 1L.

2.2. Instruments

The voltammetry and amperometric experiments were carried out using a Sama 500 potentistat/golvanostat in connection with a three-electrode system. Also, a saturated Ag/AgCl electrode as a reference electrode, a platinum wire as a counter electrode, and FeCu-LDH@Fe_3O_4/GCE as a working electrode were used. X-ray diffraction analysis was performed with a PANalytical X'Pert PRO MPD diffractometer (PANalytical company, Netherlands), equipped with monochromatized Cu Kα radiation (λ= 1.5406 A) at a voltage of 40 kV and a 40 mA current. The Fourier transform-infrared (FT-IR) spectrophotometer was used to record the FT-IR spectra from KBr pellets by VERTEX 70/70v FT-IR (Bruker, Germany) in the frequency range of 400–4000 cm^{-1}. The size and the morphology of synthesized nanocomposites were studied by a field emission scanning electron microscope ((Philips XL-30) at an accelerating voltage of 17 kV. Sonication was performed by a 50/60 Hz, 350W ultrasonic bath (EURONDA S.P.A., Italy). Measurements of pH were carried out using a digital pH meter (Mettler Toledo, model M225, Switzerland).

2.3. Synthesis of Fe_3O_4@SiO_2

The Fe_3O_4 nanoparticles were synthesized according to the co-precipitation method [26]. In summary, $FeCl_3.6H_2O$ and $FeCl_2.4H_2O$ were added in deionized water under a nitrogen atmosphere, so the ammonia solution (3 mL, 30 % v/v) was added into the solution for 30 min. The Fe_3O_4 nanoparticles were formed in this solution under heating at 85° C for 1 h. The nanoparticles were washed with the mixture of deionized water and ethanol (1:1 v/v) for several times. The resulting Fe_3O_4 nanoparticles were isolated and sonicated in 1-propanol for 30 min. Then, Ammonia solution and distillated water were added to the above solution under sonication for 1 h. To increase the magnetic nanoparticles stability, they were coated with SiO_2. Therefore, 15 mL of

TEOS was added to this solution and sonicated for 1 h at 50 °C. Finally, the Fe_3O_4@SiO_2 nanoparticles were isolated, washed three times with ethanol and dried (60° C, 24 h).

2.4. Synthesis of FeCu-LDH@Fe_3O_4

The synthesis of FeCu-LDH@Fe_3O_4 nanocomposite was carried out on the basis of the previously recommended method [27]. Briefly, Fe_3O_4@SiO_2 was dispersed into aqueous methanol water (1:1 v/v, 60 mL) and sonicated for dispersion. The pH of this solution was adjusted by NaOH solution at 9.5-10. Also, the desired amounts of $CuCl_2.2H_2O$ and $FeCl_3.6H_2O$ were dissolved in decarbonated and deionized water and were added drop by drop to the above mentioned solution with a pH in the range of 9.5-10. The resulting slurry was refluxed at 70° C for 24 h under vigorous stirring. Finally, an external magnetic field was used for collection of the synthesized Cu-Fe LDH@Fe_3O_4, and final sediment was washed with deionized water three times and dried at 50 °C overnight.

2.5. Preparation of Fe-Cu LDH@Fe_3O_4/GCE

The GCE was first freed from every contaminant by careful polishing on alumina slurry and Buehler polishing cloth. Ultrasonic rinsing and water were used to remove the alumina residues from the GCE electrode surface. Then, the as-prepared electrode was allowed to be dried in air at ambient temperature and was immediately modified with 6 µL of FeCu LDH/Fe_3O_4 nanocomposite (2 mg mL^{-1}). After GCE was dried, the FeCu-LDH@Fe_3O_4/GCE became ready for subsequent electrochemical experiments. In this method, the modifier (LDH composite) was stabilized fast and easily by physical adsorption on the electrode surface (drop casting) through intermolecular interactions such as Van Der Waals forces, Hydrogen bonding, π-π interactions, etc.

2.6. Standard solutions and real samples

Stock solutions of H_2O_2 (100 mM) were daily prepared in water and stored at 4.0 °C. Working solutions were made by dilution of a certain amount of the stock solution. In addition, the milk sample was obtained from local market and was diluted 5 times with phosphate buffer solution (0.1 mol L^{-1}, pH 7.0). It was then spiked with given concentrations of H_2O_2.

3. RESULT AND DISCUSSION

3.1. Structure and morphology characterization

Morphology and FESEM images of Cu-Fe LDH@Fe_3O_4 with the point energy dispersive X-ray spectroscopy (EDS) analysis and EDS image mapping of the elements were shown in Fig. 1(a-h). In Fig. 1a, average thickness and length of layers in the structure were obtained as approximately 35 nm and 200 nm, respectively, using the image J software. The observed accumulation in this image is probably due to the presence of magnetic nanoparticles.

In order to prove the existence of CuFe-LDH@Fe_3O_4 (Cu and Fe elements) and Fe_3O_4 nanoparticles (Fe and O elements) in the structure, the point energy dispersive X-ray spectroscopy (EDS) analysis and EDS image mapping of the elements were shown in the figure. 1 (c-h). In EDS results (Fig. 1b), Fe and Cu elements were existed with amounts of Cu (22.5 wt %) and Fe (26.8%); also other elements such as O (32.3 wt%), Si (3.1%), Cl (5.49%) and C (9.9%) were in the structure. The EDS image mapping showed uniform distribution of all elements (Fig. 1c-h).

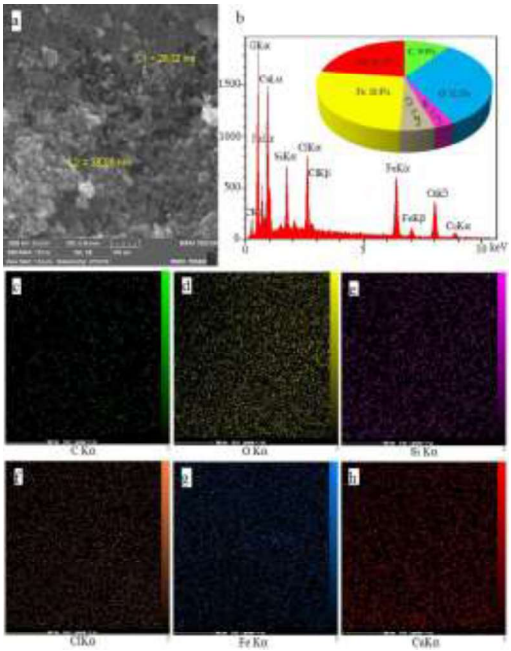

Fig. 1. (a) FESEM image of FeCu-LDH@Fe_3O_4 (b) EDS analysis of FeCu-LDH@Fe_3O_4 (c-.h) Distribution map of elements in FeCu-LDH@Fe_3O_4.

X-ray diffraction patterns of Fe_3O_4 and FeCu-LDH@Fe_3O_4 were investigated to show the structure of the nanocomposite (Fig. 2a-b). The diffraction peaks at 2θ values of 30.1 (220), 35.4 (311), 43.2 (400), 53.8 (422), 56.9 (511) and 63.0 (440) are in Fe_3O_4 XRD pattern (Fig. 2a) [28]. In Fig. 2b, the special reflection peaks, appeared at 2θ values of 16.1, 25.2, 35.039.7, 47.9, and 60.3, are related to the (003), (006), (012), (015), (018), and (110) crystal planes, respectively, which are the characteristics of LDH structure [29]. In this figure, the diffraction peaks at 2θ values of 30.1 (220), 35.4 (311), 43.2 (400), and 56.9 (511) can confirm presence of Fe_3O_4 nanoparticles in Fe-Cu LDH@Fe_3O_4 structure.

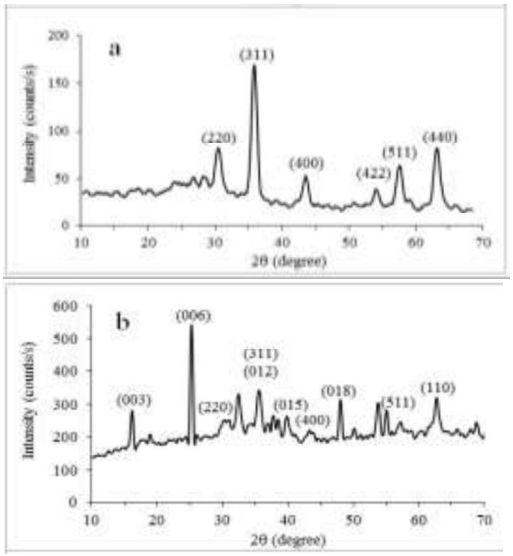

Fig. 2. XRD spectrum of Fe_3O_4 NPs and FeCu-LDH@Fe_3O_4.

The FT-IR spectra of Fe_3O_4@SiO_2 and FeCu-LDH@Fe_3O_4 were displayed in the range of 4000-400 cm^{-1} in Fig. 3a-b. The strong absorption bands at 1100 and 470 cm^{-1} (Fig. 3a) were assigned to the stretching vibration bonds in Si–O–Si and Si–O, respectively that confirmed the presence of SiO_2 followed by the iron core containing Fe_3O_4 in the structure. The peaks of Fe_3O_4 at 588 cm^{-1} were related to the vibration of Fe-O bond in Fe_3O_4 nanoparticles [30-31]. In Fig. 3b, the broad strong band at 3435 cm^{-1} was ascribed to O-H stretching vibrations of the LDH surface and interlayer water molecules that were found at a lower frequency compared with free water [32-33]. The absorption bands at 554 and 415 cm^{-1} were ascribed to M–O–H and O–M–O lattice vibrations, respectively (M is a metal (Fe and Cu)). The strong bond at 1100 cm^{-1} is weak in Fig. 2b which can confirm bonding of Si with LDH and formation of FeCu-LDH@Fe_3O_4. The weak absorption bond at 446 cm^{-1} is related to Cu–O vibrations in LDH. According to these results and all variations in two figures, it can be concluded that FeCu-LDH@Fe_3O_4 was successfully synthesized.

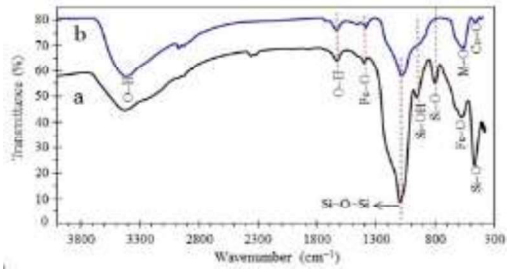

Fig. 3. FT-IR spectra of (a) Fe_3O_4 and (b) FeCu-LDH@Fe_3O_4.

3.2. Electrochemical behavior of the FeCu-LDH@Fe_3O_4/GCE

3.2.1. Cyclic voltammetric behavior of H_2O_2

To distinguish the effects of the modifier components, the electrochemical behavior of GCE and FeCu-LDH@Fe_3O_4/GCE for H_2O_2 determination were compared using cyclic voltammetry (Fig. 4). As can be seen, for the bare GCE, there was a small reduction peak, while FeCu-LDH@Fe_3O_4/GCE showed an irreversible reduction peak at -0.60 V with an obvious current increase compared with the bare electrode.

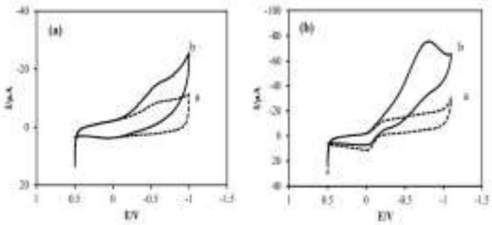

Fig. 4. The CV responses of (**a**) blank solution and (**b**) 50 μM H_2O_2 on a: bare GCE, and b: FeCu-LDH@Fe_3O_4/GCE in 0.1 M phosphate buffer (pH 7.0) at 50 mV/s scan rate.

The enhancement, observed in electro-reduction peak current of H_2O_2 on the FeCu-LDH@Fe_3O_4/GCE, can be explained by an increase in specific surface area, electrocatalytic effect and an improvement in conductivity.

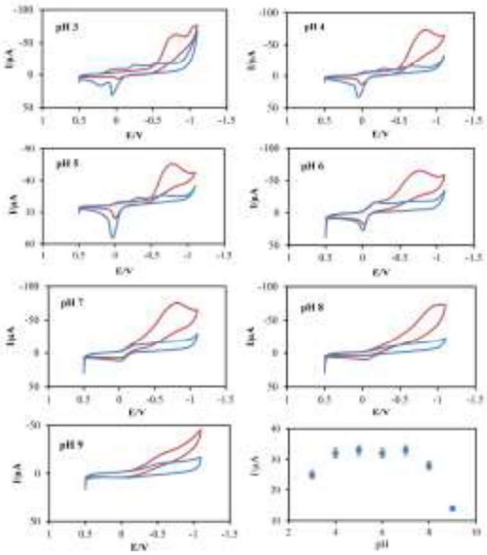

Fig. 5. The CV response of FeCu-LDH@Fe_3O_4/GCE in the presence of 50 μM H_2O_2 at 50.0 mV s^{-1} scan rate at various pHs from 3.0 to 9.0 and the plot of cathodic peak current of H_2O_2 at FeCu-LDH@Fe_3O_4/GCE *vs.* pH.

In general, the electrocatalytic oxidation of H_2O_2 on the surface of electrode can be occurred through an EC' mechanism as follows [34]:

$$Cu(II) \rightarrow Cu(III) \quad (1)$$

$2Cu(III) + H_2O_2 + 2OH^- \rightarrow 2Cu(II) + O_2 + H_2O$ (2)

Moreover, the presence of Fe in bimetallic LDH can provide more catalytic active sites and the synergistic effect, which more promote the above electrochemical oxidation.

3.2.2. Effect of pH

The pH of electrolyte is an important variable in electrocatalytic processes. In this work, pH effect was investigated in the range of 3.0 to 9.0, and the results were shown in Fig. 5. As can be seen, as the pH of electrolyte increases from 3.0 to 7.0, electro-reduction peak currents of H_2O_2 on FeCu-LDH@Fe_3O_4/GCE go up which is followed with a slight decrease in the range of 8.0 to 9.0. Therefore, pH 7.0 was selected in subsequent experiments.

3.2.3. Influence of the amount of FeCu-LDH@Fe_3O_4

It has been proved that the amount of modifier has a significant effect on electrochemical responses of modified electrodes. To maximize the results, different amounts of the FeCu-LDH@Fe_3O_4 were investigated in the range of 2 to 10 µL (2 mg mL^{-1}) on the peak current of H_2O_2 (50 µM). The results showed that the electrochemical signals significantly depended on the modifier amount on the electrode surface. According to the results, electrocatalytic peak currents increased by drop casting of the different amounts of FeCu-LDH@Fe_3O_4 up to 6 µL. However, when the FeCu-LDH@Fe_3O_4 amounts were higher than 6 µL, the electrocatalytic currents did not significantly change. Hence, a GCE coated with 6 µL of FeCu-LDH@Fe_3O_4 was used for subsequent experiments.

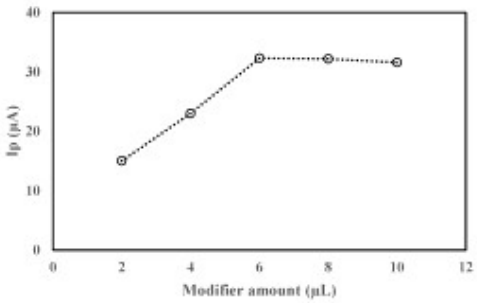

Fig. 6. Influence of the amount of FeCu-LDH@Fe_3O_4.

3.2.4. Influence of scan rate

In order to investigate the electrode reaction mechanism, the effect of potential scan rate (ν) on the peak potential and the peak current was studied in different scan rates. According to the results, as scan rates increase, catholic peak currents go up (Fig. 7). Also, a good linearity between peak currents and square root of scan rates was observed with high correlation coefficient. These results show that electro-reduction of H_2O_2 on FeCu-LDH@Fe_3O_4/GCE is controlled under diffusion mechanism according to the following equation [11]:

$I_P = 6.6621\ v^{1/2} - 7.1694$ ($R^2 = 0.9986$)

Furthermore, the reduction peak potentials were shifted toward more negative values which were expected for an irreversible electrode reaction [11].

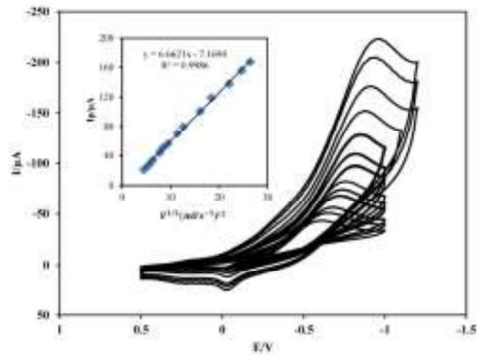

Fig. 7. The CV responses of 50 µM H_2O_2 on FeCu-LDH@Fe_3O_4/GCE in 0.1 M phosphate buffer (pH 7.0) at various scan rates (5 to 400 mV/s). Inset: plot of the peak current versus the square root of scan rate.

3.3. Analytical performance

To test the practical applicability of the FeCu-LDH@Fe_3O_4/GCE, different analytical parameters such as linear range, limit of detection, stability, repeatability, and reproducibility were studied. It was observed that the reduction peak current of H_2O_2 increases with an increment in its concentration within the range of 2 to 400 µM in two linear ranges of 2-50 µM and 50-400 µM (Fig. 8).

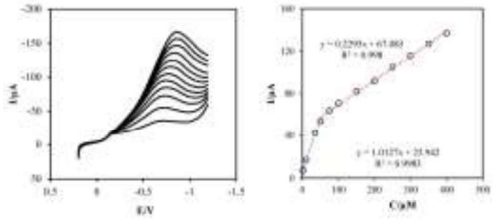

Fig. 8. The DPV responses of FeCu-LDH@Fe_3O_4/GCE in 0.1 M phosphate buffer at pH 7.0 with different concentrations of H_2O_2 (2-400 µM), Inset: plot of the peak current versus concentration of H_2O_2.

The limit of detection for FeCu-LDH@Fe_3O_4/GCE was calculated to be 0.60 µM, based on signal-to-noise ratio of 3. To investigate the repeatability of the response of the FeCu-LDH@Fe_3O_4/GCE toward H_2O_2 detection, five CV experiments were repeated consecutively on the same condition. The relative standard deviation was calculated to be 4.63%, indicating great repeatability of the responses of the FeCu-LDH@Fe_3O_4/GCE. In the next experiment, CV responses of five different independently prepared

FeCu-LDH@Fe_3O_4/GCEs were performed under the same experimental conditions. The obtained RSD% of 5.78% showed high reproducibility of the FeCu-LDH@Fe_3O_4/GCE. The stability of FeCu-LDH@Fe_3O_4/GCE was investigated by recording the CV responses of 50 µM H_2O_2 within ten days. After ten days, just 6% decrease of the signal was observed in H_2O_2 reduction signal that confirms good stability of FeCu-LDH@Fe_3O_4/GCE.

Table 1: Determination of H_2O_2 in milk samples.

Sample	Spiked (µM)	Found (µM)a	RSD (%)	Recovery (%)
1	5.00	4.88	6.78	97.60
2	25.00	25.44	6.43	101.76
3	50.00	49.20	4.76	98.40
4	175.00	174	5.12	99.43

a Average of three determinations.

In addition, the proposed FeCu-LDH@Fe_3O_4/GCE was applied for determination of H_2O_2 in milk samples. Here, milk samples were analyzed using the DPV method. Then, the milk samples were spiked with 5, 25, 50, and 175 µM of H_2O_2 and analyzed by DPV at the FeCu-LDH@Fe_3O_4/GCE. The results of recoveries and RSDs for the spiked milk samples are summarized in Table 1.

Table 2: Comparison of different modified electrodes for H_2O_2 determination.

Electrode	LOD (µg/L)	Linear Range	Ref.
GCE/Au-GS	10.0	0.03-5000	[35]
SPCE/GS-afion/Fe_3O_4-Au-HRP	12.0	0.02-2500	[36]
AgNP/rGO/GCE	31.3	100 - 100000	[37]
AgNP/GN-R/GCE	28	100 - 40000	[38]
Cu2O–rGO/GCE	21.7	30 - 12800	[39]
Fe_3O_4@C-Cu/GCE	32.6	80-372000	[40]
Hb-MCMS/GCE	21	69 - 3000	[41]
Fe/CA/CPE	500	1000-50000	[42]
Ni/[(Fe(CN)6]$^{3-}$/CPE	340	600 -6000 , 17000-54000	[43]
G/Fe_4POM–poly(1,8 DAN)/GO	2000	Up to 50000	[44]
α_2 - $K_7P_2W_{17}VO_{62}$/GCE	40	100–20000	[45]
FeCu-LDH@Fe_3O_4/GCE	0.6	2-400	This work

According to the results, recoveries, obtained in the range of 97.80% to 101.76 %, indicate that the developed sensor is reliable for the quantification of H_2O_2 in milk samples without a substantial matrix effect.

Finally, figure of merits of the proposed electrode for H_2O_2 determination and some reported sensors by others were compared (Table 2) [35-45]. As can be seen, the responses of the FeCu-LDH@Fe_3O_4/GCE were comparable to those of the reported sensors in terms of linear dynamic range and limit of detection.

4. CONCLUSION

In this research, the construction of FeCu-LDH@Fe_3O_4/GCE and its application for H_2O_2 determination were described. To achieve this goal, operative parameters in the electrochemical detection were completely studied and optimized. The proposed sensor illustrated very sensitive results in comparison with those of the bare GCE. Remarkable current sensitivity and low limit of detection of the FeCu-LDH@Fe_3O_4/GCE for the detection of H_2O_2 can provide promising sensing applications compared with unmodified and other enzyme based reported sensors in the real samples.

ACKNOWLEDGEMENTS

Financial support from the Research Affairs of University of Zabol is gratefully appreciated (grant number UOZ-GR-9718-18).

CONFLICT OF INTERESTS

The authors declare no conflict of interest.

REFERENCES

[1] A.P. Periasamy, Y.H. Ho and S.M. Chen, Multiwalled carbon nanotubes dispersed in carminic acid for the development of catalase based biosensor for selective amperometric determination of H_2O_2 and iodate, *Biosens. Bioelectron* 29 (2011) 151-158.

[2] Q. Li, W. Gao, X. Zhang, H. Liu, M. Dou, Z. Zhang and F. Wang, Mesoporous NiO nanosphere: a sensitive strain sensor for determination of hydrogen peroxide, *RSC Advances* 8 (2018) 13401-13407.

[3] K. Takeda, H. Nojima, K. Kuwahara, R.C. Chidya, A.O. Adesina and H. Sakugawa, Nanomolar determination of hydrogen peroxide in coastal seawater based on the fenton reaction with terephthalate, *Anal. Sci* 34 (2018) 459-464.

[4] J. Liang, M. Wei, Q. Wang, Z. Zhao, A. Liu, Z. Yu and Y. Tian, Sensitive electrochemical determination of hydrogen peroxide using copper nanoparticles in a polyaniline film on a glassy carbon electrode, *Anal. Lett* 51 (2018) 512-522.

[5] K. Nakano, T. Honda, K. Yamasaki, Y. Tanaka, K. Taniguchi, R. Ishimatsu and T. Imato, Carbon quantum dots as fluorescent component in peroxyoxalate

chemiluminescence for hydrogen peroxide determination, *Bull. Chem. Soc. Jpn* 91 (2018) 1128-1130.

[6] R. Pourfaraj, S.Y. Kazemi, S.J. Fatemi and P. Biparva, Synthesis of α- and β-CoNi binary hydroxides nanostructures and luminol chemiluminescence study for H_2O_2 detection, *J. Photochem. Photobiol. A: Chem* 364 (2018) 534-541.

[7] F. Zarif, S. Rauf, M.Z. Qureshi, N. Samad Shah, A. Hayat, N. Muhammad, A. Rahim, M. Hasnain Nawaz and M. Nasir, Ionic liquid coated iron nanoparticles are promising peroxidase mimics for optical determination of H_2O_2, *Microchim. Acta* 185 (2018) 302.

[8] V. Gupta, P. Mahbub, P.N. Nesterenko and B. Paull, A new 3D printed radial flow-cell for chemiluminescence detection: Application in ion chromatographic determination of hydrogen peroxide in urine and coffee extracts, *Anal. Chim. Acta* 1005 (2018) 81-92.

[9] M.R. Miah and T. Ohsaka, Cathodic detection of H_2O_2 using iodide-modified gold electrode in alkaline media, *Anal. chem* 78 (2006) 1200-1205.

[10] I.L. de Mattos, L. Gorton and T. Ruzgas, Sensor and biosensor based on Prussian Blue modified gold and platinum screen printed electrodes, *Biosens. Bioelectron* 18 (2003) 193-200.

[11] H. Razmi, R. Mohammad-Rezaei and H. Heidari, Self-assembled prussian blue nanoparticles based electrochemical sensor for high sensitive determination of H_2O_2 in acidic media, *Electroanal* 21 (2009) 2355-2362.

[12] A.S. Kitte, D.B. Assresahegn and R.T. Soreta, Electrochemical determination of hydrogen peroxide at glassy carbon electrode modified with palladium nanoparticles, *J. Serb. Chem. Soc* 78 (2013) 701-711.

[13] Q. Rui, K. Komori, Y. Tian, H. Liu, Y. Luo and Y. Sakari, Electrochemical biosensor for the detection of H_2O_2 from living cancer cells based on ZnO nanosheets, *Anal. Chim. Acta* 670 (2010) 57-62.

[14] G.H. Wang and L.M. Zhang, Using novel polysaccharide– silica hybrid material to construct an amperometric biosensor for hydrogen peroxide, *J. Phys. Chem. B* 110 (2006) 24864-24868.

[15] A.A. Ensafi, M.M. Abarghoui and B. Rezaei, Electrochemical determination of hydrogen peroxide using copper/porous silicon based non-enzymatic sensor, *Sensor. Actuat. B-Chem* 196 (2014) 398-405.

[16] H. Ahmar, S. Keshipour, H. Hosseini, A.R. Fakhari, A. Shaabani and A. Bagheri, Electrocatalytic oxidation of hydrazine at glassy carbon electrode modified with ethylenediamine cellulose immobilized palladium nanoparticles, *J. Electroanal. Chem* 690 (2013) 96-103.

[17] X. Guo, F. Zhang, D.G. Evans and X. Duan, Layered double hydroxide films: synthesis, properties and applications, *Chem. Comm* 46 (2010) 5197-5210.

[18] G. Mishra, B. Dash and S. Pandey, Layered double hydroxides: A brief review from fundamentals to application as evolving biomaterials, *Appl. Clay Sci* 153 (2018) 172-186.

[19] A. Soussou, I. Gammoudi, F. Morote, A. Kalboussi, T. Cohen-Bouhancina, C. Grauby-Heywang and Z.M. Baccar, Efficient immobilization of tyrosinase enzyme on layered double hydroxide hybrid nanomaterials for electrochemical detection of polyphenols, *IEEE Sens. J* 17 (2017) 4340-4348.

[20] P. Saikia, A. Borah and R.L. Goswamee, Hybrid nanocomposites of layered double hydroxides: an update of their biological applications and future prospects, *Colloid Polym. Sci* 295 (2017) 725-747.

[21] N. Baig and M. Sajid, Applications of layered double hydroxides based electrochemical sensors for determination of environmental pollutants: a review, *Trends Environ. Anal. Chem* 16 (2017) 1-15.

[22] B. Rezaei, M. Heidarbeigy, A.A. Ensafi and M. Dinari, Electrochemical determination of papaverine on Mg-Al layered double hydroxide/graphene oxide and CNT modified carbon paste electrode, *IEEE Sens. J* 16 (2016) 3496-3503.

[23] H. Yin, L. Cui, S. Ai, H. Fan and L. Zhu, Electrochemical determination of bisphenol A at Mg–Al–CO_3 layered double hydroxide modified glassy carbon electrode, *Electrochim. Acta* 55 (2010) 603-610.

[24] R. Hushiarian, N.A.Yusof, A.H. Abdullah, S.A. Alang Ahmad and S.W. Dutse, Facilitating the indirect detection of genomic DNA in an electrochemical DNA biosensor using magnetic nanoparticles and DNA ligase, *Anal. Chem. Res* 6 (2015) 17-25.

[25] A. Zabardasti, H. Afrouzi and R.P. Talemi, A simple and sensitive methodology for voltammetric determination of valproic acid in human blood plasma samples using 3-aminopropyletriethoxy silane coated magnetic nanoparticles modified pencil graphite electrode, *Mater. Sci. Eng* C 76 (2017) 425-430.

[26] L. Adlnasab, M. Ezoddin, M. Shabanian and B. Mahjoob, Development of ferrofluid mediated CLDH@Fe_3O_4@Tanic acid- based supramolecular solvent: Application in air-assisted dispersive micro solid phase extraction for preconcentration of diazinon and metalaxyl from various fruit juice samples, *Microchem. J* 146 (2019) 1–11.

[27] M. Ezoddin, L. Adlnasab, A. Afshari kaveh, M.A. Karimi and B. Mahjoob, Development of air-assisted dispersive micro solid phase extraction based supramolecular solvent-

mediated Fe_3O_4@Cu-Fe–LDH for the determination of tramadol in biological samples, *Biomed. Chromatogr* 33 (2019) e4572.

[28] L. Yan, K. Yang, R. Shan, T. Yan, J. Wei, S. Yu, H. Yu and B. Du. Kinetic, isotherm and thermodynamic investigations of phosphate adsorption onto core–shell Fe_3O_4@LDHs composites with easy magnetic separation assistance, *J. Colloid Interface Sci* 448 (2015) 508–516.

[29] M. Laipan, H. Fu, R. Zhu, L. Sun, J. Zhu and H. He,Converting spent Cu/Fe layered double hydroxide into Cr(VI) reductant and porous carbon material, *Scientific Reports* (2017) 7: 7277, 1-11.

[30] T. Baskar, JIA Zhaohua, D. Lingmei, L. Dehua and D. Wei, Lipase NS81006 immobilized on Fe3O4 magnetic nanoparticles for biodiesel production, *Ovidius University Annals of Chemistry,* 27 (2016) 13-21.

[31] T.K. HanhTa, M.T. Trinh, N.V. Long, T.T.M. Nguyen, T.L.T. Nguyen, T.L. Thuoc, B.T. Phan, D. Mott, S. Maenosono, H. Tran-Van, V.H. Le, Synthesis and surface functionalization of Fe_3O_4@SiO_2 core-shell nanoparticles with 3-glycidoxypropyltrimethoxysilane and 1,1′-carbonyldiimidazole for bio-applications, *Colloid. Surface* 504 (2016) 376-383.

[32] Q. Zhou, M. Lei, J. Li, K. Zhao and Y. Liu, Sensitive determination of bisphenol A, 4-nonylphenol and 4-octylphenol by magnetic solid phase extraction with Fe@MgAl-LDH magnetic nanoparticles from environmental water samples, *Sep. Purifi. Technol* 182 (2017) 78-86.

[33] S. Tang, G.H. Chia and H.K. Lee, Magnetic core shell iron (II,III) oxide@layered double oxide microspheres for removal of 2,5-dihydroxybenzoic acid from aqueous solutions, *J. Colloid Interf. Sci* 437 (2015) 316-323.

[34] D.K. Yadav, V. Ganesan, R. Gupta, M. Yadav, P.K. Sonkar and P.K. Rastogi, Copper oxide immobilized clay nano architectures as an efficient electrochemical sensing platform for hydrogen peroxide, *J. Chem. Sci* 132, (2020) 1-10.

[35] P.F. Pang, Z.M. Yang, S.X. Xiao, J.L. Xie, Y.L. Zhang and Y.T. Gao, Nonenzymatic amperometric determination of hydrogen peroxide by graphene and gold nanorods nanocomposite modified electrode, *J. Electroanal. Chem* 727 (2014) 27-33.

[36] X. Yang, F.B. Xiao, H.W. Lin, F. Wu, D.Z. Chen and Z.Y. Wu, A novel H_2O_2 biosensor based on Fe_3O_4-Au magnetic nanoparticles coated horseradish peroxidase and graphene sheets-Nafion film modified screen-printed carbon electrode, *Electrochim. Acta* 109 (2013) 750-755.

[37] S. Liu, J. Tian, L. Wang and X. Sun, A method for the production of reduced graphene oxide using benzylamine as a reducing and stabilizing agent and its subsequent decoration with Ag nanoparticles for enzymeless hydrogen peroxide detection, *Carbon* 49 (2011) 3158-3164.

[38] S. Liu, J. Tian, L. Wang, H. Li, Y. Zhang and X. Sun, Stable aqueous dispersion of graphene nanosheets: noncovalent functionalization by a polymeric reducing agent and their subsequent decoration with Ag nanoparticles for enzymeless hydrogen peroxide detection, *Macromolecules* 43 (2010) 10078-10083.

[39] F. Xu, M. Deng, G. Li, S. Chen and L. Wang, Electrochemical behavior of cuprous oxide–reduced graphene oxide nanocomposites and their application in nonenzymatic hydrogen peroxide sensing, *Electrochim. Acta* 88 (2013) 59-65.

[40] M. Zhang, Q. Sheng, F. Nie and J. Zheng, Synthesis of Cu nanoparticles-loaded Fe_3O_4@ carbon core–shell nanocomposite and its application for electrochemical sensing of hydrogen peroxide. *J. Electroanal. Chem.* 730 (2014) 10-15.

[41] G.S. Lai, H.L. Zhang and D.Y. Han, A novel hydrogen peroxide biosensor based on hemoglobin immobilized on magnetic chitosan microspheres modified electrode, *Sensor. Actuat B-Chem* 129 (2008) 497-503.

[42] C.I. Fort, L.C. Cotet, V. Danciu, G.L. Turdean and I.C. Popescu, Iron doped carbon aerogel new electrode material for electrocatalytic reduction of H_2O_2, *Mater. Chem. Phys* 138 (2013) 893-898.

[43] S.A. Kitte, B.D. Assresahegn and T.R. Soreta, Electrochemical determination of hydrogen peroxide at a glassy carbon electrode modified with palladium nanoparticles, *J. Serb. Chem. Soc* 78 (2013) 701-711.

[44] G.L. Turdean, A. Curulli, I. Catalin Popescu, C. Rosu and G. Palleschi, Electropolymerized architecture entrapping a trilacunary keggin, type polyoxometalate for assembling a glucose biosensor, *Electroanalysis* 14 (2002) 1550-1556.

[45] P. Wang, X. Wang, L. Bi, G. Zhu, Sol-gel-derived α_2-$K_7P_2W_{17}VO_{62}$/graphite/ organoceramic composite as the electrode material for a renewable amperometric hydrogen peroxide sensor, *J. Electroanal. Chem* 495 (2000) 51-56.

تعیین مقدار هیدروژن پراکسید در نمونه‌های شیر برپایه الکترود گلاسی کربن اصلاح‌شده با هیدروکسید لایه‌ای دوگانه Fe/Cu و نانوذرات Fe_3O_4

عارفه گرگیج[۱]، حمید احمر[۱،*]، لاله عدل نسب[۲]

۱. گروه شیمی، دانشکده علوم، دانشگاه زابل، زابل، ایران

۲. گروه پژوهشی شیمی، پژوهشکده شیمی و پتروشیمی، پژوهشگاه استاندارد، کرج، ایران

تاریخ دریافت: ۱۱ مرداد ۱۴۰۰ تاریخ پذیرش: ۲۵ شهریور ۱۴۰۰

چکیده

هیدروژن پراکسید (H_2O_2) کاربرد گسترده‌ای در صنایع مختلف نظیر نساجی، دارویی، بالینی و مواد غذایی دارد. هیدروژن پراکسید به‌طور معمول در غلظت حدود ۶٪ استفاده می‌شود، اما در غلظت بالاتر می‌تواند اکسید کننده، خورنده و سمی باشد. در این تحقیق، یک حسگر الکتروشیمیایی جدید مبتنی بر نانوکامپوزیت هیدروکسید لایه‌ای دوگانه فلزات Cu/Fe تثبیت شده برروی بستر مغناطیسی با موفقیت ساخته شده و برای تشخیص H_2O_2 مورد استفاده قرار می‌گیرد. جهت بررسی ساختار و ویژگی نانوکامپوزیت تهیه شده از میکروسکوپ الکترونی روبشی، پراش اشعه ایکس، ولتامتری چرخه‌ای و ولتامتری پالس تفاضلی استفاده شد. سپس نانوکامپوزیت برروی الکترود کربن شیشه‌ای تثبیت و فعالیت الکتروکاتالیستی آن در احیاء H_2O_2 مورد بررسی قرار گرفت. عوامل موثر بر فعالیت الکتروکاتالیستی (مقدار اصلاح‌گر، pH محلول و زمان آنالیز) بررسی و بهینه‌سازی شد. تحت شرایط بهینه، هیدروژن پراکسید یک جریان احیایی خطی از خود نشان داد. هم‌چنین حدتشخیص ۳ میکرومولار و تکرار پذیری حسگر تهیه شده در محدوده ۲ تا ۴۰۰ میکرومولار به دست آمد. در نهایت حسگر مربوطه به‌صورت موفقیت آمیز برای تعیین هیدروژن پراکسید با محاسبه بازیابی در نمونه شیر مورد مطالعه قرار گرفت.

واژه‌های کلیدی

نانوذرات؛ هیدروژن پراکسید؛ هیدروکسید لایه‌ای دوگانه؛ حسگر الکتروشیمیایی؛ نمونه‌های شیر.